Journal of Power Sources 195 (2010) 5382–5386

Contents lists available at ScienceDirect

Journal of Power Sources

journal homepage: www.elsevier.com/locate/jpowsour

Short communication

In situ synthesis of ultra-fine, porous, tin oxide-carbon nanocomposites via a molten salt method for lithium-ion batteries

Bin Liu[a,e], Zai Ping Guo[b,a,c,*], Guodong Du[b,c], Yanna Nuli[d,c], Mohd Faiz Hassan[b,c], Dianzeng Jia[a,c]

[a] Institute of Applied Chemistry, Xinjiang University, Urumqi 830046, PR China
[b] Institute for Superconducting & Electronic Materials, University of Wollongong, NSW 2522, Australia
[c] School of Mechanical, Materials & Mechatronics Engineering, University of Wollongong, NSW 2522, Australia
[d] Department of Chemical Engineering, Shanghai Jiao Tong University, Shanghai 200240, PR China
[e] School of Science, Xinjiang Eduction Institute, Urumqi, Xinjiang, PR China

ARTICLE INFO

Article history:
Received 13 November 2009
Received in revised form 23 February 2010
Accepted 25 February 2010
Available online 16 March 2010

Keywords:
Ultra-fine, porous, tin oxide-carbon nanocomposites
Molten salt
Anode
Lithium-ion battery

ABSTRACT

Ultra-fine, porous, tin oxide–carbon (SnO_2/C) nanocomposites are fabricated by a molten salt method at 300 °C, and malic acid is decomposed as the carbon source. In situ synthesis is favourable for the combination of carbon and SnO_2. The structure and morphology are confirmed by X-ray diffraction analysis, specific surface-area measurements, and transmission electron microscopy (TEM). Examination of TEM images reveals that the SnO_2 nanoparticles are embedded in the carbon matrix, with sizes between 2 and 5 nm. The electrochemical measurements show that the nanocomposite delivers a high capacity with good capacity retention as an anode material for lithium-ion batteries, due to the combination of the ultra-fine porous structure and the carbon component.

1. Introduction

Lithium-ion batteries are key power sources for mobile communication devices, portable electronic devices, and even upcoming electric and hybrid electric vehicles. To achieve lithium-ion batteries with high specific energy and long cycling performance, a great deal of effort has been made to develop new electrode materials or design novel electrode material structures [1–3]. For anode materials, various nanocrystalline oxides have been extensively investigated in order to replace the commonly used carbonaceous materials. Among them, tin oxide (SnO_2) stands out, due to its high storage capacity (theoretical capacity 781 mAh g^{-1}) and its suitable operating voltage, both of which are lower than those of cobalt oxide (Co_3O_4), nickel oxide (NiO) and other transition metal oxides, but higher than that of graphite, thus improving the safety of batteries and delivering a high working cell voltage.

The practical use of SnO_2 anode materials has been frustrated by their poor capacity retention due to the volume change of tin (Sn) (~200%) during the lithium alloying/de-alloying process and a large initial irreversible capacity caused by lithium oxide (Li_2O) formation. In order to alleviate its electrochemical disadvantages, much attention has been paid to the morphological and structural modification of SnO_2 [4–7]. Recently, for example, various SnO_2 nanostructures have been designed to improve the electrochemical performance [8–12]. These synthesis methods, however, usually suffer from disadvantages related to high cost, low production output and tedious synthetic procedures that may prevent them from being used in large-scale applications. Another way to improve the electrochemical performance of tin-based anode materials is to introduce inactive, or less active, compositions to buffer the volume change [13,14]. Carbon, as a conductive material, has been reported to improve SnO_2 capacity retention [15–17].

It is obvious that a high content of small SnO_2 particles, as well as very high amalgamation between the carbon and the SnO_2, will greatly contribute to the further enhancement of the electrochemical performance of SnO_2 electrodes. In previous work [18], ultra-fine porous SnO_2 materials, were successfully fabricated and exhibited excellent cycling stability compared with the other SnO_2 electrodes reported to date. In this study, carbon is incorporated in ultra-fine porous SnO_2 and in situ synthesis of SnO_2/C nanocomposites is achieved by a simple molten salt method at 300 °C. The combination of the large viscosity and high dielectric constant of the eutectic system with a low synthesis temperature (300 °C) results in very fine nanoparticles (2–5 nm). In addition, the in situ preparation process gives better results

* Corresponding author at: Institute for Superconducting & Electronic Materials, University of Wollongong, NSW 2522, Australia. Tel.: +61 2 4221 5225; fax: +61 2 4221 5731.
E-mail address: zguo@uow.edu.au (Z.P. Guo).

0378-7753/$ – see front matter © 2010 Elsevier B.V. All rights reserved.
doi:10.1016/j.jpowsour.2010.02.084

than subsequent carbon coating and leads to complete amalgamation and good interface affinity between the SnO_2 and the carbon and thereby ensures structural stability of the composite during discharge–charge cycling.

2. Experimental

2.1. Sample preparation

A molten salt method was employed to synthesize the SnO_2/C nanocomposite. Lithium hydroxide monohydrate (Aldrich), lithium nitrate (Aldrich), hydrogen peroxide (Sigma–Aldrich), malic acid, and tin (II) chloride dehydrate (Analar-BDH) were used as starting materials. 100 mmol of lithium nitrate, 100 mmol of lithium hydroxide monohydrate, 10 mmol of tin (II) chloride dehydrate and 10 mmol of malic acid were mixed in an agate mortar to obtain a homogenous composition. Then, 50 mmol of hydrogen peroxide was added to the mixture and stirred for 24 h. The mixture was then heated at 120 °C for 4 h in a vacuum oven, followed by further heat-treatment in air at 300 °C for 3 h in a muffle furnace. After cooling in air, the SnO_2/C nanocomposite was separated from the eutectic mixture by washing with a large amount of de-ionized water and by filtration. The product was dried under vacuum at 60 °C for 24 h. As a comparison, bare SnO_2 nanopowders were prepared by the same method in the absence of malic acid.

2.2. Sample characterization

Precise carbon contents in the as-prepared composite were determined by thermogravimetric and differential thermal analysis (TGA/DTA) with a Setaram 92 equipment. The powders were characterized by X-ray diffraction (XRD, Philips PW1730) with Cu Kα radiation, scanning electron microscopy (SEM, JEOL JEM-3000), transmission electron microscopy (TEM, JEOL 2011) and specific surface-area measurements (Brunauer–Emmett–Teller (BET) surface area, ASAP2010). The TEM samples were prepared by deposition of ground particles on to lacy carbon support films.

2.3. Electrochemical measurements

Coin cells were made to test the electrochemical performance. The electrode was prepared by mixing as-prepared nano-SnO_2 or SnO_2/C nanocomposite as active material with 10 wt.% carbon black (Super P, MMM, Belgium) and 10 wt.% polyvinylidene fluoride (PVDF) binder in N-methyl-2-pyrrolidinone (NMP) solvent to form a homogeneous slurry, which was then spread on copper foil. The coated electrodes (average thickness of ~50 μm) were dried in a vacuum oven at 110 °C for 24 h and then pressed. Electrochemical measurements were carried out using CR 2032 coin-type cells that were assembled in an argon-filled glove-box (Mbraun, Unilab, Germany) by stacking a porous polypropylene separator containing liquid electrolyte between the composite electrode and a lithium foil counter electrode. The electrolyte used was 1 M $LiPF_6$ in a 50:50 (v/v) mixture of ethylene carbonate (EC) and dimethyl carbonate (DMC), provided by MERCK KgaA, Germany. The cells were galvanostatically charged and discharged in different voltage ranges at a constant current density of 100 mA g^{-1}. Cyclic voltammetry measurements were conducted with a CHI 660B Electrochemical Workstation at a scanning rate of 0.1 mV s^{-1}. All the electrochemical tests were carried out at room temperature (25 °C).

3. Results and discussion

The XRD pattern of the C–SnO_2 nanocomposite is compared in Fig. 1 with that of the SnO_2 nanopowder prepared by the molten salt method. All reflections for both samples are in good agreement with a tetragonal rutile structure (JCPDS 41-1445), belonging to the space group $P4_2/mnm$ (136). There is no notable peak shifting or significant intensity variation between the C–SnO_2 and the bare SnO_2 samples. The highly broadened peaks indicate that the as-prepared SnO_2 and C–SnO_2 are composed of SnO_2 crystallites of very small size. The calculated mean crystallite sizes of SnO_2 estimated from Scherrer's formula are 3.6 and 4.1 nm for the bare SnO_2 and the C–SnO_2 nanocomposite, respectively, based on the (1 1 0), (1 0 1), and (2 1 1) peaks.

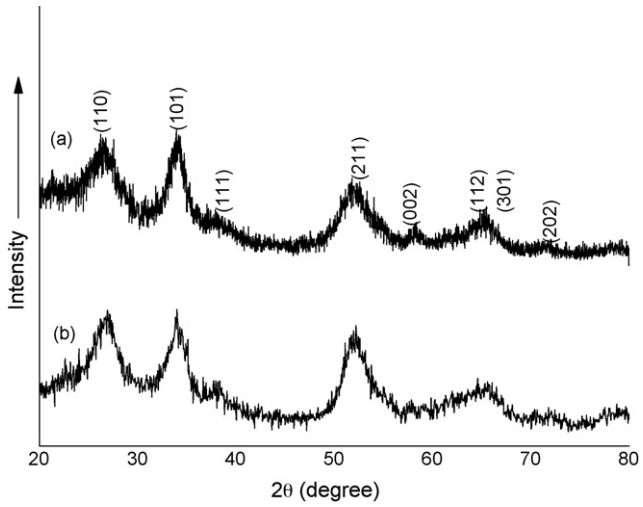

Fig. 1. X-ray diffraction patterns of (a) C–SnO_2 nanocomposite compared with (b) SnO_2 nanopowders.

According to the results of thermogravimetric (TG) analysis, the weight percentage of amorphous carbon in the as-prepared composite is about 12 wt.%. Transmission electron microscope (TEM) images of SnO_2 and the SnO_2/C composite at different magnifications are displayed in Fig. 2. Very fine nanoparticles are formed and are rather monodisperse. Furthermore, there are large numbers of pores several nanometers in size among the particles. BET analysis shows that the SnO_2/C nanocomposite possesses a slightly larger pore size and volume, as illustrated in Table 1. These pores provide void space to accommodate the volume expansion during Li^+ insertion [11,19]. High-resolution TEM images clearly show lattice fringes, with individual crystallite sizes between 2 and 5 nm. The SnO_2 nanoparticles in the SnO_2/C nanocomposite are dispersed in an amorphous carbon matrix (Fig. 2(d)). The lattice fringes have spacings of about 0.32 and 0.27 nm, corresponding to the (1 1 0) and (1 0 1) planes of SnO_2, respectively. The indexed ring patterns (inset of Fig. 2(d)) are consistent with the X-ray diffraction patterns (Fig. 1), and the blurred ring patterns can be derived from the amorphous carbon phase.

To test the potential applicability of the as-prepared ultra-fine porous SnO_2/C nanocomposite in lithium-ion batteries, the electrochemical performance of SnO_2/C nanocomposite electrodes was systematically investigated. The cyclic voltammetry (CV) curves of the SnO_2/C composite are compared with those of bare nano-SnO_2 in Fig. 3. The CV profiles for the bare nano-SnO_2 electrode show a

Table 1
Specific surface-area measurements using low-temperature liquid nitrogen absorption.

	SnO_2	SnO_2/C
BET surface area (m^2 g^{-1})	158.4017	125.7393
Pore volume (cm^3 g^{-1})	0.079797	0.103043
Average pore width (nm)	2.01506	3.27798

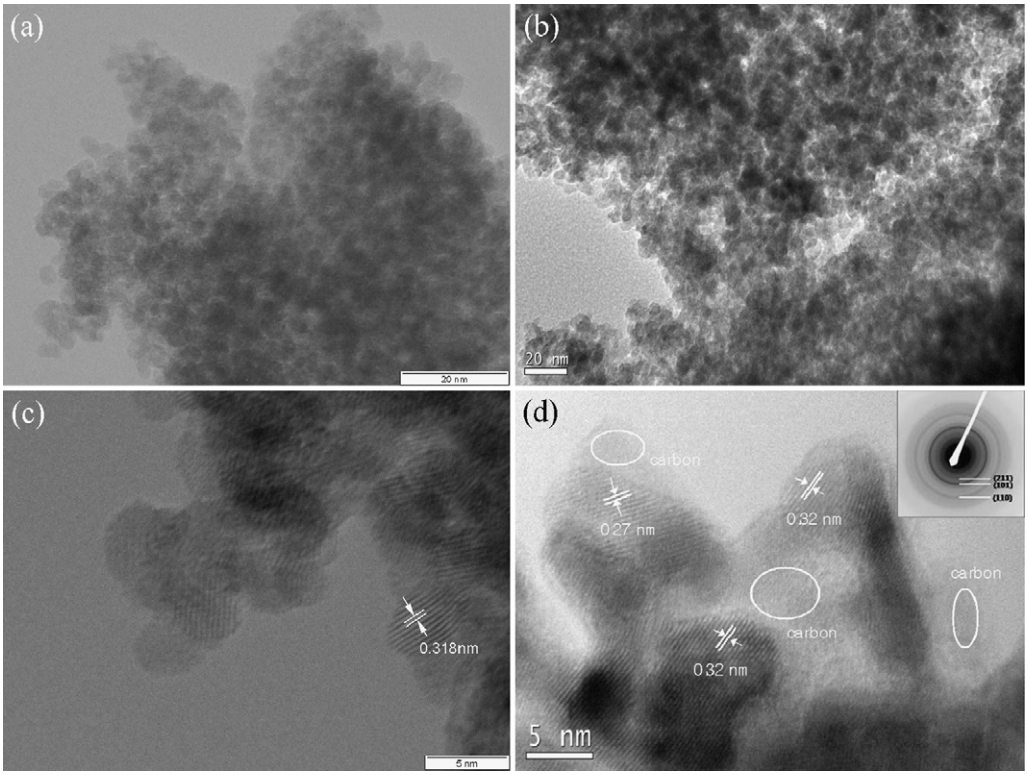

Fig. 2. TEM images of (a and c) bare SnO_2 and (b and d) SnO_2/C nanocomposite prepared by molten salt method. Indexed diffraction pattern (inset in (d)) confirms presence of SnO_2 nanoparticles. High-resolution TEM image (d) shows SnO_2 nanoparticles embedded in amorphous carbon matrix.

wide reduction peak from 0.7 to 1.1 V, which can be ascribed to the decomposition of SnO_2 to Sn and Li_2O composite (Eq. (1)), and the formation of a solid electrolyte interphase (SEI, Eq. (2)). These reactions cause a large initial irreversible capacity during the first cycle of the bare SnO_2 electrode. Another pair of reduction and oxidation peaks at around 0.2 and 0.6 V is related to the formation of Li_xSn, as described in Eq. (3) [14,20–22].

$$SnO_2 + 4Li^+ + 4e^- \rightarrow Sn + 2Li_2O \quad (1)$$

$$Li^+ + e^- + \text{electrolyte} \rightarrow \text{SEI(Li)} \quad (2)$$

$$Sn + xLi^+ + xe^- \leftrightarrow Li_xSn \quad (0 \le x \le 4.4) \quad (3)$$

It is generally accepted that the first two reactions are not reversible and are thus responsible for the large irreversible capacity of the first cycle [6,23]. The alloying reaction between Sn and Li is highly reversible, as verified by the observation of an oxidation peak at around 0.5 V. It should be noted that another oxidation peak at around 1.3 V is also observed, which is most likely due to the partly reversible reaction of Eq. (1), because the Li–Sn alloying/de-alloying reactions only occur below 1.0 V [3,4]. For the SnO_2/C nanocomposite electrode, the peak corresponding to the formation of the SEI film is significantly weaker and may shift to a lower voltage, which indicates that a carbon/electrolyte interface layer is also formed in addition to the Sn|electrolyte interface layer [24]. The shape of the reduction peak at around 0.2 V is quite different for SnO_2/C compared with that for the bare SnO_2 and thereby suggests that the carbon component also participates in the electrochemical reactions. By comparing the CV curves of the SnO_2/C nanocomposite electrode with those of bare SnO_2, it is also found that the intensity of the peaks remains more stable during cycling and this demonstrates the higher reversibility of the nanocomposite electrode.

The first discharge (Li insertion)–charge (Li extraction) curves of the SnO_2/C nanocomposite and the bare SnO_2 electrodes were obtained in the voltage range of 0.01–3 V at a current density of

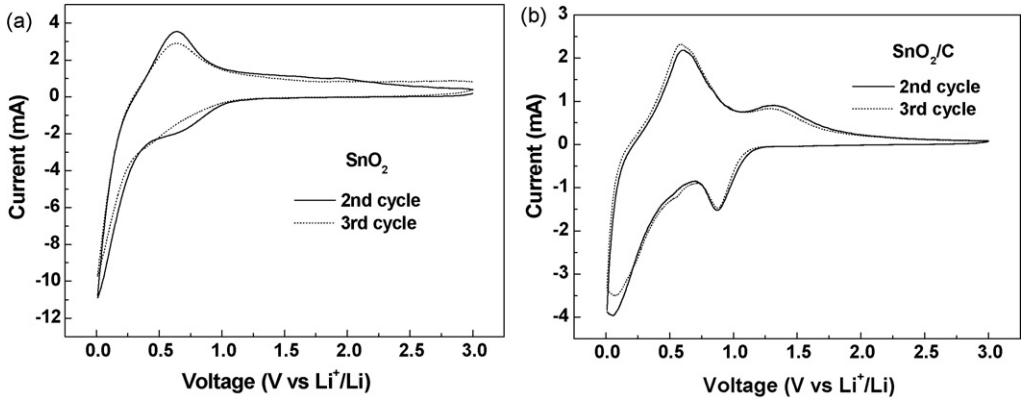

Fig. 3. Cyclic voltammograms of bare SnO_2 and SnO_2/C composite.

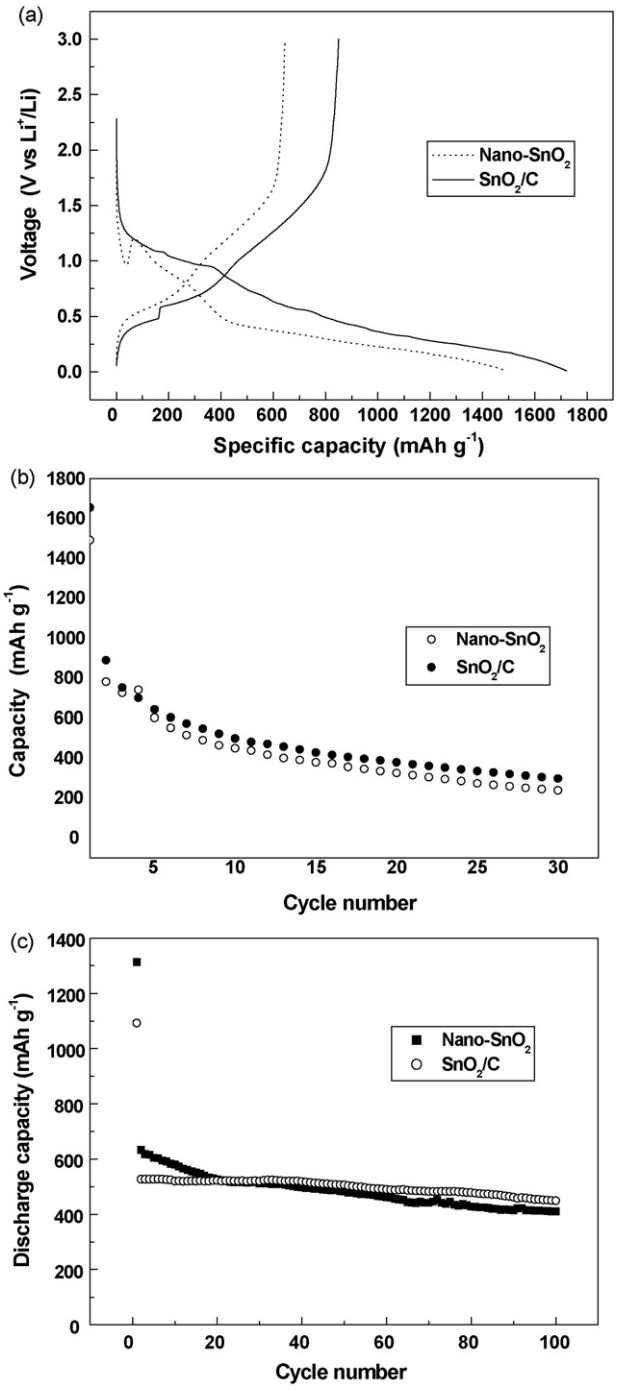

Fig. 4. (a) First discharge–charge curves for SnO_2/C and bare SnO_2 samples cycled at 100 mA g^{-1}. (b) Cycling performance of two samples cycled between 0.01 and 3 V. (c) Discharge capacities of SnO_2/C composite and bare nano-SnO_2 anodes vs. cycle number, cycled between 0.05 and 1.5 V.

100 mA g^{-1} (Fig. 4(a)). The SnO_2/C nanocomposite shows a much higher reversible capacity (848 mAh g^{-1}) than the bare nano-SnO_2 (643 mAh g^{-1}), where the specific capacities are calculated with respect to the weight of active materials. Furthermore, the SnO_2/C nanocomposite exhibits an initial coulombic efficiency of about 50%, which is remarkably higher than that of bare nano-SnO_2 (43.2%). When the voltage is limited to the 0.05–1.5 V range, both the bare SnO_2 and SnO_2/C composite give much better cycling performance, with a reversible capacity of 410.1 and 449.7 mAh g^{-1}, respectively, after 100 cycles. Moreover, the composite has a good initial coulombic efficiency of 70.6% and better capacity retention (85.3%) than either bare nano-SnO_2 (64.8%) (as shown in Fig. 4(c)) or other such types of SnO_2, alone or in composite form, that have been reported in the literature. It is believed that the improved initial coulombic efficiency of the SnO_2/C nanocomposite can be attributed to fewer non-bonding terminations of Sn atoms or O atoms on the surface of the SnO_2, as well as to the enhancement of the charge transport induced by the carbon component [17].

Compared with reported data, the electrochemical performance of the as-prepared SnO_2 nanopowder is excellent, owing to the ultra-fine nanosized porous structure. Nanosize particles result in a lower absolute volume change and shorter Li diffusion lengths, while pores accommodate volume change and promote electrolyte diffusion [25,26]. Nevertheless, the electrochemical performance of the SnO_2/C composite is much superior compared with that of bare SnO_2 prepared by the same method, which could be attributed to: (i) the high distribution of oxide particles within the carbon matrix and the good interface affinity between oxide and carbon particles, which resulted from the in situ preparation of the oxide and carbon; (ii) the carbon matrix, which not only improves the conductivity of the SnO_2 anode but also effectively buffers the volume expansion of Sn during lithium intercalation and hinders tin aggregation during cycling.

4. Conclusions

A simple molten salt method been developed for in situ preparation of an ultra-fine porous SnO_2/C nanocomposite. The good interface affinity between the carbon matrix and the SnO_2 particles and the effective buffer presented by the carbon results in significant improvement in the electrochemical performance of the as-prepared SnO_2/C nanocomposite as an anode material for lithium-ion batteries. The SnO_2/C nanocomposite has a good initial coulombic efficiency of 70.6% when the electrodes are cycled in the voltage range of 0.05–1.5 V, which is remarkably higher than that of bare nano-SnO_2 (41.1%) fabricated by the same method. Moreover, the nanocomposite shows better capacity retention (85.3%) than bare nano-SnO_2 (64.8%) after 100 cycles. The as-prepared SnO_2/C nanocomposites could be a good anode material for commercial lithium-ion batteries. In addition, the simple molten salt synthesis method used in this study involves no templates or surfactants, and has the added advantage of a shorter synthesis time, so that it is a promising method for industrial application.

Acknowledgements

Financial support provided by the Australian Research Council (ARC) through an ARC Discovery project (DP0878611) is gratefully acknowledged. In addition, the authors thank Dr. Tania Silver at the University of Wollongong for critical reading of the manuscript.

References

[1] J.M. Tarascon, Nature 414 (2001) 359–367.
[2] J.R. Dahn, T. Zheng, Y.H. Liu, J.S. Xue, Science 270 (1995) 590–593.
[3] M. Winter, J.O. Besenhard, M.E. Spahr, P. Novak, Adv. Mater. 10 (1998) 725–763.
[4] Y. Idota, T. Kubota, A. Matsufuji, Y. Maekawa, T. Miyasaka, Science 276 (1997) 1395–1397.
[5] I.A. Courtney, J.R. Dahn, J. Electrochem. Soc. 144 (1997) 2045–2052.
[6] J.O. Besenhard, J. Yang, M. Winter, J. Power Sources 68 (1997) 87–90.
[7] L. Yuan, Z.P. Guo, K. Konstantinov, H.K. Liu, S.X. Dou, J. Power Sources 159 (2006) 345–348.
[8] V. Juttukonda, R.L. Paddock, J.E. Raymond, D. Denomme, A.E. Richardson, L.E. Slusher, J. Am. Chem. Soc. 128 (2006) 420–421.
[9] B. Cheng, J.M. Russell, W.S. Shi, L. Zhang, E.T. Samulski, J. Am. Chem. Soc. 126 (2004) 5972–5973.
[10] L. Zhao, M. Yosef, M. Steinhart, P. Goring, H. Hofmeister, U. Gosele, Angew. Chem. Int. Ed. 45 (2006) 311–315.

[11] X.W. Lou, Y. Wang, C. Yuan, J.Y. Lee, L.A. Archer, Adv. Mater. 18 (2006) 2325–2329.
[12] J. Ba, J. Polleux, M. Antonietti, M. Niederberger, Adv. Mater. 17 (2005) 2509–2512.
[13] J. Yang, Y. Takeda, N. Imanishi, O. Yamamoto, J. Electrochem. Soc. 146 (1999) 4009–4013.
[14] J. Hassoun, S. Panero, P. Simon, P.L. Taberna, B. Scrosati, Adv. Mater. 19 (2007) 1632–1635.
[15] Z.P. Guo, Z.W. Zhao, H.K. Liu, S.X. Dou, Carbon 43 (2005) 1392–1399.
[16] G.M. An, N. Na, X.R. Zhang, Z.J. Miao, S.D. Miao, K.L. Ding, Nanotechnology 18 (2007) 435707.
[17] M.S. Park, Y.M. Kang, J.H. Kim, G.X. Wang, S.X. Dou, H.K. Liu, Carbon 46 (2008) 35–40.
[18] Z.P. Guo, G.D. Du, Y. Nuli, M. Hossan, H.K. Liu, J. Mater. Chem. 19 (2009) 3253.
[19] L. Yuan, Z.P. Guo, K. Konstantinov, J.Z. Wang, H.K. Liu, Electrochim. Acta 51 (2006) 3680–3684.
[20] G. Derrien, J. Hassoun, S. Panero, B. Scrosati, Adv. Mater. 19 (2007) 2336–2340.
[21] I.A. Courtney, J.R. Dahn, J. Electrochem. Soc. 144 (1997) 2943–2948.
[22] L.H. Shi, H. Li, Z.X. Wang, X.J. Huang, L.Q. Chen, J. Mater. Chem. 11 (2001) 1502–1505.
[23] O. Mao, R.A. Dunlap, J.R. Dahn, J. Electrochem. Soc. 146 (1999) 405–413.
[24] S.H. Ng, J.Z. Wang, D. Wexler, K. Konstantinov, Z.P. Guo, H.K. Liu, Angew. Chem. Int. Ed. 45 (2006) 6896–6899.
[25] N. Pereira, L.C. Klein, G.G. Amatucci, Solid State Ionics 167 (2004) 29.
[26] Y. Wang, I. Djerdj, B. Smarsly, M. Antonietti, Chem. Mater. 21 (2009) 3202.